Analytical Solutions for the Optimal Reference Currents for MTPC/MTPA, MTPV and MTPF Control of Anisotropic Synchronous Machines

Hisham Eldeeb[1], Christoph M. Hackl[1,*], Julian Kullick[1], Lorenz Horlbeck[2]
[1]Research group "Control of Renewable Energy Systems" (CRES), Technical University of Munich, Garching, Germany
[2]Institute of Automotive Technology (FTM), Technical University of Munich, Garching, Germany

***Abstract*—Analytical solutions for the optimal current references during maximum torque per current (MTPC; or maximum torque per Ampere (MTPA)), maximum torque per voltage (MTPV) and maximum torque per flux (MTPF) operation of anisotropic synchronous machines with *non-negligible* stator resistance and mutual inductance are presented. The analytical solutions allow for an (almost) instantaneous computation of the corresponding reference currents without neglecting stator resistance and/or mutual inductance (as usually done). Numerical methods (approximating these solutions only) are *no longer* required. The derived analytical solutions for MTPC, MTPV and MTPF operation are suitable for any anisotropic synchronous machine; even for nonlinear reluctance synchronous machines, as the presented measurement results illustrate.**

NOTATION

$\mathbb{N}, \mathbb{R}, \mathbb{C}$: natural, real and complex numbers. $\operatorname{sign}(x) := \begin{cases} 1 & , x > 0 \\ 0 & , x = 0 \\ -1 & , x < 0 \end{cases}$: sign function. $\boldsymbol{x} := (x_1, \dots, x_n)^\top \in \mathbb{R}^n$: column vector, $n \in \mathbb{N}$ where "$^\top$" and ":=" mean "transposed" (interchanging rows and columns of a matrix or vector) and "is defined as", resp., $\mathbf{0}_n \in \mathbb{R}^n$: zero vector. $\boldsymbol{a}^\top \boldsymbol{b} := a_1 b_1 + \dots + a_n b_n$: scalar product of the vectors $\boldsymbol{a} := (a_1, \dots, a_n)^\top$ and $\boldsymbol{b} := (b_1, \dots, b_n)^\top$. $\|\boldsymbol{x}\| := \sqrt{\boldsymbol{x}^\top \boldsymbol{x}} = \sqrt{x_1^2 + \dots + x_n^2}$: Euclidean norm of $\boldsymbol{x}$. $\boldsymbol{A} \in \mathbb{R}^{n \times n}$: (square) matrix with n rows and columns. $\boldsymbol{A}^{-1}$: inverse of $\boldsymbol{A}$ (if exists). $\boldsymbol{I}_n \in \mathbb{R}^{n \times n} := \operatorname{diag}(1, \dots, 1)$: identity matrix.

I. INTRODUCTION AND MOTIVATION

Electrical machines consume more than half of the globally generated electricity [1]. Hence, advances in research on the optimal feedforward torque control problem of electric drives (machine+inverter) have been made; in particular for synchronous machines (SMs) with non-negligible anisotropy such as *interior permanent-magnet (PM) synchronous motors (IPMSMs)*, *reluctance synchronous machines (RSMs)*, *PM-assisted RSMs (PMA-RSMs)* or *PM-enhanced RSMs (PME-RSMs)* [2], [3]. The optimal feedforward torque control problem has been investigated in numerous publications, see e.g. [4], [5], [6], [7], [8] to name a few. The online computation of the optimal reference currents for the different operation strategies such as MTPC, MTPV or MTPF is usually done *numerically* or *analytically but with simplifying assumptions (e.g. neglecting stator resistance and/or cross-coupling inductance)* imposed on the machine model or the physical constraints (e.g. voltage ellipse). Numerical solutions, in general, increase the computational load on the real-time system. Analytical solutions are more attractive, since they are easier to implement, more accurate and faster to compute. However, to the best knowledge of the authors, analytical solutions *including* stator resistance *and* mutual inductance for MTPC, MTPV and MTPF of anisotropic SMs are not available. For example, in [9, Sec. IV] and [10, Sec. 2.2.3], it was stated that acquiring a general analytical solution of the optimal currents for MTPV and MTPF while considering stator resistance and magnetic cross-coupling seems *not possible* due to the high degree of complexity. A preliminary result on MTPC with analytical solution for the reference currents, which also considers the cross-coupling inductance, was recently published in [11]. The main contributions of the present paper are: (i) The derivation of analytical solutions of the optimal reference currents for MTPC, MTPV and MTPF operation incorporating *stator resistance* and *cross-coupling (mutual) inductance*. The proposed analytical solutions offer (i-a) guaranteed convergence to the optimal reference currents (compared to numerical methods), (i-b) easy/straight-forward implementation, and (i-c) low computational burden allowing for an implementation even on modest (hence cheap) processor boards; (ii) The analytical solutions for the optimal reference currents are obtained by (ii-a) the use of *Lagrangian multipliers* and (ii-b) an *implicit* problem formulation as *quadrics* (i.e. all trajectories of constraints and operation strategies in the (d, q)-plane–such as e.g. current circle, voltage ellipse and torque hyperbola–are reformulated implicitly as quadric surfaces); and (iii) the negative effects of neglecting stator resistance and mutual inductance or both on the optimality of all operation strategies are illustrated, which show that neglecting these two parameters during optimization will lead to significant deviations between optimal and approximated reference currents and, therefore, to decreased efficiency.

*All authors contributed equally to the paper. Corresponding author is C.M. Hackl (christoph.hackl@tum.de).

II. Problem formulation and mathematical preliminaries

First, the steady-state model and the operation constraints of the considered synchronous machines, and the problem formulation are presented. Then, the machine torque and all operation constraints (such as current or voltage limit) are reformulated *implicitly* as *quadratic surfaces (quadrics)*. These implicit forms will pave the way for the analytical solutions of the reference currents for MTPC, MTPV or MTPF operation.

A. Steady-state model of generic synchronous machines (SMs)

The steady-state model of anisotropic SMs in the synchronously rotating $k=(d,q)$-reference frame is given by

$$\boldsymbol{u}_\mathrm{s}^k = R_\mathrm{s}\boldsymbol{i}_\mathrm{s}^k + \omega_\mathrm{k}\boldsymbol{J}\boldsymbol{L}_\mathrm{s}^k\boldsymbol{i}_\mathrm{s}^k + \omega_\mathrm{k}\boldsymbol{J}\boldsymbol{\psi}_\mathrm{pm}^k, \tag{1}$$

where $\boldsymbol{J} := \left[\begin{smallmatrix}0 & -1\\ 1 & 0\end{smallmatrix}\right]$ and a (locally) *constant* inductance matrix $\boldsymbol{L}_\mathrm{s}^k := \left[\begin{smallmatrix}L_\mathrm{s}^d, & L_\mathrm{m}\\ L_\mathrm{m}, & L_\mathrm{s}^q\end{smallmatrix}\right] \in \mathbb{R}^{2\times 2}$ (e.g. obtained by linearizing the nonlinear flux linkage around the actual operating point) was assumed such that the (local approximation of the) flux linkage can be expressed by

$$\left.\begin{aligned}\boldsymbol{\psi}_\mathrm{s}^k(\boldsymbol{i}_\mathrm{s}^k) &= \boldsymbol{L}_\mathrm{s}^k\boldsymbol{i}_\mathrm{s}^k + \boldsymbol{\psi}_\mathrm{pm}^k \quad \text{where}\\ \boldsymbol{\psi}_\mathrm{pm}^k &= \begin{pmatrix}\psi_\mathrm{pm}^d\\ \psi_\mathrm{pm}^q\end{pmatrix} = \begin{cases}(\psi_\mathrm{pm},0)^\top, & \text{for PMSM and PME-RSM [3],}\\ (0,-\psi_\mathrm{pm})^\top, & \text{for PMA-RSM [3], [2], and}\\ (0,0)^\top, & \text{for RSM [3], [12].}\end{cases}\end{aligned}\right\} \tag{2}$$

The machine torque is then given by

$$\begin{aligned} m_\mathrm{m}(\boldsymbol{i}_\mathrm{s}^k) &\overset{(2)}{=} \tfrac{3}{2}n_\mathrm{p}\left[(\boldsymbol{i}_\mathrm{s}^k)^\top\boldsymbol{J}\boldsymbol{L}_\mathrm{s}^k\boldsymbol{i}_\mathrm{s}^k + (\boldsymbol{i}_\mathrm{s}^k)^\top\boldsymbol{J}\boldsymbol{\psi}_\mathrm{pm}^k\right]\\ &= \tfrac{3}{2}\,n_\mathrm{p}\Big[\psi_\mathrm{pm}^d i_\mathrm{s}^q - \psi_\mathrm{pm}^q i_\mathrm{s}^d + \big(L_\mathrm{s}^d - L_\mathrm{s}^q\big)i_\mathrm{s}^d i_\mathrm{s}^q\\ &\qquad + L_\mathrm{m}\big((i_\mathrm{s}^q)^2 - (i_\mathrm{s}^d)^2\big)\Big]. \end{aligned} \tag{3}$$

In (1), (2) and (3), R_s (in Ω) is the stator resistance, $\boldsymbol{u}_\mathrm{s}^k := (u_\mathrm{s}^d, u_\mathrm{s}^q)^\top$ (in V), $\boldsymbol{i}_\mathrm{s}^k := (i_\mathrm{s}^d,\, i_\mathrm{s}^q)^\top$ (in A) and $\boldsymbol{\psi}_\mathrm{s}^k := (\psi_\mathrm{s}^d,\, \psi_\mathrm{s}^q)^\top$ (in Wb) are stator voltage, current and flux linkage vectors, respectively. Note that $\omega_\mathrm{k} = n_\mathrm{p}\,\omega_\mathrm{m}$ (in $\mathrm{rad/s}$) is the *electric* angular frequency, whereas ω_m is the *mechanical* angular frequency of the machine and n_p denotes the number of pole pairs. The inductance matrix $\boldsymbol{L}_\mathrm{s}^k = \left[\begin{smallmatrix}L_\mathrm{s}^d, & L_\mathrm{m}\\ L_\mathrm{m}, & L_\mathrm{s}^q\end{smallmatrix}\right] = (\boldsymbol{L}_\mathrm{s}^k)^\top > 0$ depends on stator inductances $L_\mathrm{s}^q > 0$, $L_\mathrm{s}^d > 0$ (both in H) and cross-coupling (mutual) inductance $L_\mathrm{m} \in \mathbb{R}$ (in H) satisfying $L_\mathrm{s}^d L_\mathrm{s}^q - L_\mathrm{m}^2 > 0$. The permanent-magnet flux linkage is denoted by $\boldsymbol{\psi}_\mathrm{pm}^k = (\psi_\mathrm{pm}^d,\, \psi_\mathrm{pm}^q)^\top$.

Remark II.1. *Equation* (2) *implies a constant inductance matrix; this is in line with most recent publications which also deal with constant inductances only (see e.g. [6], [7]). This simplification will* not *be true in general [12]. Nevertheless, in the humble opinion of the authors, the presented results are of quite some relevance and have not been discussed in this general framework before: The results of this paper can be considered as a generalization of the results for IPMSM in [5] to* any *anisotropic SM (e.g. PMA/PME-RSMs and RSMs) with non-negligible stator resistance R_s and mutual inductance L_m. Moreover, in Section IV, measurement results will illustrate applicability to a nonlinear RSM.*

B. Operation constraints and Problem formulation

Stator current and voltage vectors should never exceed their respective maximal *magnitudes* $\hat{\imath}_\mathrm{max} > 0$ (in A) and $\hat{u}_\mathrm{max} > 0$ (in V; both are amplitudes *not* RMS values here). Hence, the following must be ensured by the control system for all time

$$\begin{aligned} \|\boldsymbol{i}_\mathrm{s}^k\|^2 = (i_\mathrm{s}^d)^2 + (i_\mathrm{s}^q)^2 \le \hat{\imath}_\mathrm{max}^2 \text{ and}\\ \|\boldsymbol{u}_\mathrm{s}^k\|^2 = (u_\mathrm{s}^d)^2 + (u_\mathrm{s}^q)^2 \le \hat{u}_\mathrm{max}^2. \end{aligned} \tag{4}$$

For a given reference torque $m_\mathrm{m,ref}$ (in $\mathrm{N\,m}$), the general objective is to find optimal and analytical solutions for the reference currents for MTPC, MTPV and MTPF operation. The following general optimization problem

$$\begin{aligned} \max_{\boldsymbol{i}_\mathrm{s}^k} \; -f(\boldsymbol{i}_\mathrm{s}^k) \;\; \text{s.t.} \;\; &\|\boldsymbol{u}_\mathrm{s}^k\| \le \hat{u}_\mathrm{max},\; \|\boldsymbol{i}_\mathrm{s}^k\| \le \hat{\imath}_\mathrm{max},\\ &|m_\mathrm{m}(\boldsymbol{i}_\mathrm{s}^k)| \le |m_\mathrm{m,ref}| \;\text{ and}\\ &\operatorname{sign}(m_\mathrm{m,ref}) = \operatorname{sign}(m_\mathrm{m}(\boldsymbol{i}_\mathrm{s}^k)), \end{aligned} \tag{5}$$

with three inequality constraints and one equality constraint must be solved online, where obviously the sign of reference and machine torque should coincide. The function $f(\boldsymbol{i}_\mathrm{s}^k)$ depends on the operation strategy (e.g. $f(\boldsymbol{i}_\mathrm{s}^k) = \|\boldsymbol{i}_\mathrm{s}^k\|^2$ for MTPC; for more details, see Sec. III). The most favorable outcome is an analytical solution to the optimization problem (5) for the optimal reference current vector

$$\boldsymbol{i}_\mathrm{s,ref}^k(m_\mathrm{m,ref}, \hat{u}_\mathrm{max}, \hat{\imath}_\mathrm{max}, \omega_\mathrm{k}) := \arg\max\nolimits_{\boldsymbol{i}_\mathrm{s}^k} -f(\boldsymbol{i}_\mathrm{s}^k), \tag{6}$$

which is then handed over to the underlying current control.

C. Implicit formulation of torque & constraints as quadrics

The steady-state model (1) will be the basis for the upcoming derivations. The trick to obtain and derive analytical solutions for the reference currents for MTPC, MTPV or MTPF operation is the reformulation of the general optimization problem (5) *implicitly by quadrics (or quadric surfaces)* which will allow to invoke the Lagrangian formalism. In the next subsections, the implicit forms of torque hyperbola, voltage ellipse (elliptical area), current circle (circular area) and flux norm are presented. Stator resistance $R_\mathrm{s} \neq 0$ and mutual inductance $L_\mathrm{m} \neq 0$ will *not* be neglected to present the most general result.

1) Torque hyperbola (constant torque trajectory): To derive the quadric (implicit form) of the torque hyperbola, define

$$\left.\begin{aligned}\boldsymbol{T} &:= \tfrac{3}{4}n_\mathrm{p}\big(\boldsymbol{J}\boldsymbol{L}_\mathrm{s}^k + \boldsymbol{L}_\mathrm{s}^k\boldsymbol{J}^\top\big) = \tfrac{3}{2}n_\mathrm{p}\begin{bmatrix}-L_\mathrm{m} & \frac{L_\mathrm{s}^d - L_\mathrm{s}^q}{2}\\ \frac{L_\mathrm{s}^d - L_\mathrm{s}^q}{2} & L_\mathrm{m}\end{bmatrix} = \boldsymbol{T}^\top,\\ \boldsymbol{t} &:= \tfrac{3}{4}n_\mathrm{p}\boldsymbol{J}\boldsymbol{\psi}_\mathrm{pm}^k \;\text{ and }\; \tau(m_\mathrm{m,ref}) := -m_\mathrm{m,ref}.\end{aligned}\right\} \tag{7}$$

Moreover, note that $(\boldsymbol{i}_\mathrm{s}^k)^\top\boldsymbol{J}\boldsymbol{L}_\mathrm{s}^k\boldsymbol{i}_\mathrm{s}^k = (\boldsymbol{i}_\mathrm{s}^k)^\top\boldsymbol{L}_\mathrm{s}^k\boldsymbol{J}^\top\boldsymbol{i}_\mathrm{s}^k$, hence $\frac{3}{4}n_\mathrm{p}(\boldsymbol{i}_\mathrm{s}^k)^\top(\boldsymbol{J}\boldsymbol{L}_\mathrm{s}^k + \boldsymbol{L}_\mathrm{s}^k\boldsymbol{J}^\top)\boldsymbol{i}_\mathrm{s}^k = (\boldsymbol{i}_\mathrm{s}^k)^\top\boldsymbol{T}\boldsymbol{i}_\mathrm{s}^k$. Now, by combining (7) and the relations above with (3), the machine torque can be written as follows

$$m_\mathrm{m}(\boldsymbol{i}_\mathrm{s}^k) = (\boldsymbol{i}_\mathrm{s}^k)^\top\boldsymbol{T}\boldsymbol{i}_\mathrm{s}^k + 2\boldsymbol{t}^\top\boldsymbol{i}_\mathrm{s}^k;$$

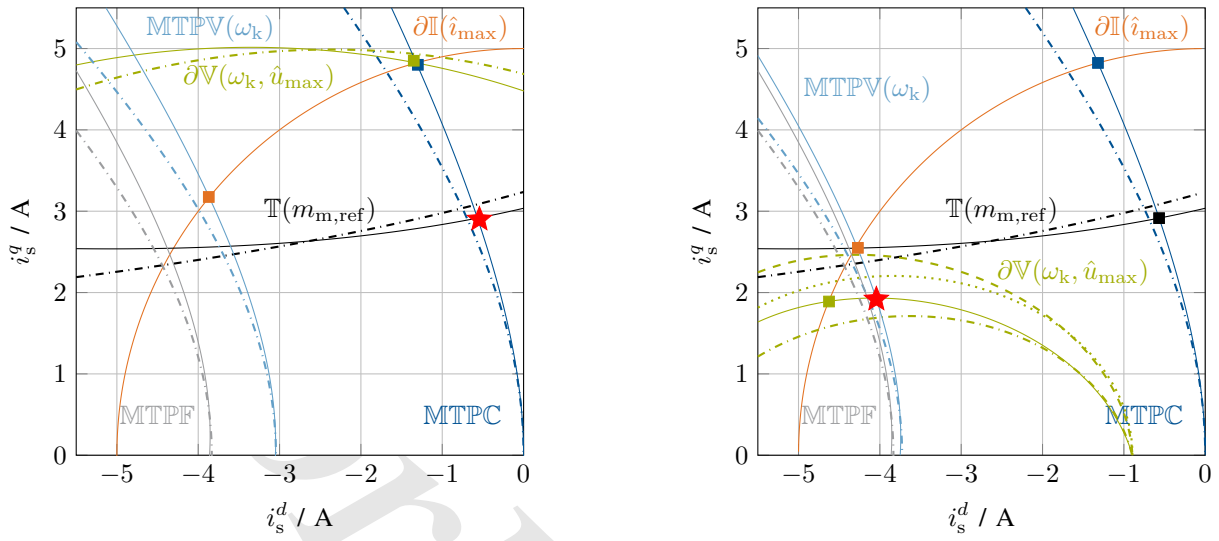

(a) *MTPC, i.e.,* $\mathbb{MTPC} \cap \mathbb{T}(m_{\mathrm{m,ref}})$, *for* $\omega_k = \omega_{k,nom}$.

(b) *MTPV, i.e.,* $\mathbb{MTPV}(\omega_k) \cap \partial\mathbb{V}(\omega_k, \hat{u}_{max})$, *for* $\omega_k = 3\omega_{k,nom}$.

Fig. 1: *Illustration of impact of* neglecting *stator resistance (dashed line:* $R_s = 0$*), mutual inductance (dash-dotted:* $L_m = 0$*) or both (dotted:* $R_s = L_m = 0$*)) on the MTPC and MTPV operation strategy: The plots show voltage ellipse* —$\partial\mathbb{V}(\omega_k, \hat{u}_{max})$, - - $\partial\mathbb{V}(\omega_k, \hat{u}_{max}; R_s = 0)$, -·- $\partial\mathbb{V}(\omega_k, \hat{u}_{max}; L_m = 0)$, ··· $\partial\mathbb{V}(\omega_k, \hat{u}_{max}; R_s = L_m = 0)$, *max. current circle* —$\partial\mathbb{I}(\hat{\imath}_{max})$, *MTPC hyperbola* —$\mathbb{MTPC}$, -·- $\mathbb{MTPC}(L_m = 0)$, *torque hyperbola* —$\mathbb{T}(m_{m,ref})$, -·- $\mathbb{T}(m_{m,ref}; L_m = 0)$, *MTPV hyperbola* —$\mathbb{MTPV}(\omega_k)$, -·- $\mathbb{MTPV}(\omega_k; L_m = 0)$, *MTPF hyperbola* —$\mathbb{MTPF}$, -·- $\mathbb{MTPF}(L_m = 0)$ *and optimal operation point* ★.

which, for a given *constant* reference torque $m_{m,ref}$ and (7), can be expressed implicitly as *machine torque hyperbola* (a quadric) as follows

$$\mathbb{T}(m_{m,ref}) := \left\{ \boldsymbol{i}_s^k \in \mathbb{R}^2 \;\middle|\; (\boldsymbol{i}_s^k)^\top \boldsymbol{T} \boldsymbol{i}_s^k + 2\boldsymbol{t}^\top \boldsymbol{i}_s^k + \tau(m_{m,ref}) = 0 \right\}. \tag{8}$$

An exemplary torque hyperbola is plotted in Fig. 1 (see black line —in Fig. 1).

2) Voltage elliptical area (reformulation of the voltage constraint in (4)*):* Inserting (1) into (4) and squaring the result yields an expression of the voltage constraint in (4) which can be written implicitly as quadric surface (for details see [13])

$$\begin{aligned} \mathbb{V}(\omega_k, \hat{u}_{max}) := \{\, & \boldsymbol{i}_s^k \in \mathbb{R}^2 \mid \\ & (\boldsymbol{i}_s^k)^\top \boldsymbol{V}(\omega_k)\, \boldsymbol{i}_s^k + 2\, \boldsymbol{v}(\omega_k)^\top \boldsymbol{i}_s^k + \nu(\omega_k, \hat{u}_{max}) \le 0 \}, \end{aligned}$$

with the following matrix, vector and scalar

$$\left.\begin{aligned} \boldsymbol{V}(\omega_k) &:= R_s^2 \boldsymbol{I}_2 + R_s \omega_k \left(\boldsymbol{J} \boldsymbol{L}_s^k + \boldsymbol{L}_s^k \boldsymbol{J}^\top \right) + \omega_k^2 (\boldsymbol{L}_s^k)^2 \\ &= \omega_k^2 \begin{bmatrix} \frac{R_s^2}{\omega_k^2} - 2\frac{R_s L_m}{\omega_k} + (L_s^d)^2 + L_m^2, & \frac{R_s}{\omega_k}(L_s^d - L_s^q) + L_m(L_s^d + L_s^q) \\ \frac{R_s}{\omega_k}(L_s^d - L_s^q) + L_m(L_s^d + L_s^q), & \frac{R_s^2}{\omega_k^2} + 2\frac{R_s L_m}{\omega_k} + (L_s^q)^2 + L_m^2 \end{bmatrix}, \\ \boldsymbol{v}(\omega_k)^\top &:= \omega_k \left(\boldsymbol{\psi}_{pm}^k\right)^\top \left(\omega_k \boldsymbol{L}_s^k + R_s \boldsymbol{J}^\top \right) \quad \text{and} \\ \nu(\omega_k, \hat{u}_{max}) &:= \omega_k^2 \left(\boldsymbol{\psi}_{pm}^k\right)^\top \boldsymbol{J}^\top \boldsymbol{J} \boldsymbol{\psi}_{pm}^k - \hat{u}_{max}^2. \end{aligned}\right\} \tag{9}$$

$\mathbb{V}(\omega_k, \hat{u}_{max})$ describes the *voltage elliptical area*. Its boundary, the *voltage ellipse* (green line —in Fig. 1), is given by

$$\begin{aligned} \partial\mathbb{V}(\omega_k, \hat{u}_{max}) := \{\, & \boldsymbol{i}_s^k \in \mathbb{R}^2 \mid \\ & (\boldsymbol{i}_s^k)^\top \boldsymbol{V}(\omega_k)\, \boldsymbol{i}_s^k + 2\, \boldsymbol{v}(\omega_k)^\top \boldsymbol{i}_s^k + \nu(\omega_k, \hat{u}_{max}) = 0 \}. \end{aligned} \tag{10}$$

Since $\boldsymbol{V}(\omega_k) = \boldsymbol{V}(\omega_k)^\top$, $\boldsymbol{v}(\omega_k)$ and $\nu(\omega_k, \hat{u}_{max})$ explicitly depend on the electric angular velocity ω_k, the voltage ellipse itself depends on ω_k, and, hence, will move within the current loci for varying angular velocities (see Fig. 1).

3) Current circular area (reformulation of the current constraint in (4)*):* The current constraint in (4) can also be expressed implicitly as quadric as follows

$$\mathbb{I}(\hat{\imath}_{max}) := \left\{ \boldsymbol{i}_s^k \in \mathbb{R}^2 \;\middle|\; (\boldsymbol{i}_s^k)^\top \boldsymbol{I}_2 \boldsymbol{i}_s^k - \hat{\imath}_{max}^2 \le 0 \right\},$$

which describes the admissible *maximum current circular area*: The magnitude of the stator current vector must not exceed the current limit $\hat{\imath}_{max}$ (permanently). The *maximum current circle* (see orange line —in Fig. 1), i.e. the boundary of $\mathbb{I}(\hat{\imath}_{max})$, is given by

$$\partial\mathbb{I}(\hat{\imath}_{max}) := \left\{ \boldsymbol{i}_s^k \in \mathbb{R}^2 \;\middle|\; (\boldsymbol{i}_s^k)^\top \boldsymbol{I}_2 \boldsymbol{i}_s^k - \hat{\imath}_{max}^2 = 0 \right\}. \tag{11}$$

4) Norm of the flux linkage: To operate the machine in MTPF mode, the squared norm of the flux linkage is minimized. The flux norm can also be expressed as quadric as follows

$$\begin{aligned} \|\boldsymbol{\psi}_{pm}^k\|^2 &\overset{(2)}{=} (\boldsymbol{L}_s^k \boldsymbol{i}_s^k + \boldsymbol{\psi}_{pm}^k)^\top (\boldsymbol{L}_s^k \boldsymbol{i}_s^k + \boldsymbol{\psi}_{pm}^k) \\ &=: (\boldsymbol{i}_s^k)^\top \boldsymbol{F} \boldsymbol{i}_s^k + 2\boldsymbol{f} \boldsymbol{i}_s^k + \phi, \end{aligned} \tag{12}$$

with the following corresponding matrix, vector and scalar

$$\left.\begin{aligned} \boldsymbol{F} &:= (\boldsymbol{L}_s^k)^2 = \begin{bmatrix} (L_s^d)^2 + L_m^2 & L_m(L_s^d + L_s^q) \\ L_m(L_s^d + L_s^q) & (L_s^q)^2 + L_m^2 \end{bmatrix} = \boldsymbol{F}^\top, \\ \boldsymbol{f} &:= \boldsymbol{L}_s^k \boldsymbol{\psi}_{pm}^k, \quad \text{and} \quad \phi := (\boldsymbol{\psi}_{pm}^k)^\top \boldsymbol{\psi}_{pm}^k = \|\boldsymbol{\psi}_{pm}^k\|^2. \end{aligned}\right\} \tag{13}$$

III. Operation Strategies

Now, MTPC, MTPV and MTPF operation are discussed, the analytical solutions for the respective reference currents are

presented, and the impact of neglecting stator resistance and mutual inductance on the efficiency is illustrated (see Fig. 1).

A. Maximum-Torque-per-Current (MTPC) hyperbola (with L_m)

For low speeds, the voltage constraint in (4) is *not* critical. The minimization of (copper) losses dominates the operation of the machine and the MTPC strategy should be used. The MTPC optimization problem is formulated as follows

$$\max_{\boldsymbol{i}_\mathrm{s}^k\in\mathbb{S}} -\|\boldsymbol{i}_\mathrm{s}^k\|^2 \;\text{ s.t. } m_\mathrm{m}(\boldsymbol{i}_\mathrm{s}^k) = (\boldsymbol{i}_\mathrm{s}^k)^\top \boldsymbol{T}\boldsymbol{i}_\mathrm{s}^k + 2\boldsymbol{t}^\top(\boldsymbol{i}_\mathrm{s}^k) \stackrel{!}{=} m_{\mathrm{m,ref}} \tag{14}$$

with $\mathbb{S} := \mathbb{V}(\omega_\mathrm{k},\hat{u}_\mathrm{max}) \cap \mathbb{I}(\hat{\imath}_\mathrm{max})$. Its solution, the MTPC hyperbola (see blue line ——in Fig. 1), can be expressed as quadric

$$\mathbb{MTPC} := \big\{\, \boldsymbol{i}_\mathrm{s}^k \in \mathbb{R}^2 \;\big|\; (\boldsymbol{i}_\mathrm{s}^k)^\top \boldsymbol{M}_\mathrm{C}\, \boldsymbol{i}_\mathrm{s}^k + 2\,\boldsymbol{m}_\mathrm{C}^\top \boldsymbol{i}_\mathrm{s}^k = 0\big\}. \tag{15}$$

The derivation of the implicit form (15) is presented in Appendix B of [13]. Note that the presented derivation can also be applied to obtain the implicit forms of the two other operation strategies such as MTPV or MTPF (for details see [13]).

Remark III.1 (MTPC versus MTPA)**.** *In most publications, the MTPC strategy is called Maximum Torque Per Ampere (MTPA). From a physical point of view, the use of physical quantities (like torque and current) seems more appropriate than a mixture of quantity and unit (like torque and Ampere). Therefore, here, the terminology MTPC will be adopted.*

B. Maximum-Torque-per-Voltage (MTPV) hyperbola (with R_s and L_m)

For high speeds, the voltage constraint in (4) is critical and dominates the operation of the machine. Now, the operation strategy is MTPV. The corresponding MPTV optimization problem is formulated as follows

$$\max_{\boldsymbol{i}_\mathrm{s}^k\in\mathbb{S}} -\|\boldsymbol{u}_\mathrm{s}^k(\boldsymbol{i}_\mathrm{s}^k)\|^2 \text{ s.t. } m_\mathrm{m}(\boldsymbol{i}_\mathrm{s}^k) = (\boldsymbol{i}_\mathrm{s}^k)^\top \boldsymbol{T}\boldsymbol{i}_\mathrm{s}^k + 2\boldsymbol{t}^\top(\boldsymbol{i}_\mathrm{s}^k) \stackrel{!}{=} m_{\mathrm{m,ref}} \tag{16}$$

with $\mathbb{S} = \mathbb{V}(\omega_\mathrm{k},\hat{u}_\mathrm{max}) \cap \mathbb{I}(\hat{\imath}_\mathrm{max})$. Its solution, the MTPV hyperbola, depends on ω_k and is implicitly given by the quadric (for details see [13])

$$\begin{aligned}\mathbb{MTPV}(\omega_\mathrm{k}) := \big\{\, &\boldsymbol{i}_\mathrm{s}^k \in \mathbb{R}^2 \;\big|\\ &(\boldsymbol{i}_\mathrm{s}^k)^\top \boldsymbol{M}_\mathrm{V}(\omega_\mathrm{k})\, \boldsymbol{i}_\mathrm{s}^k + 2\,\boldsymbol{m}_\mathrm{V}(\omega_\mathrm{k})^\top \boldsymbol{i}_\mathrm{s}^k + \mu_\mathrm{V}(\omega_\mathrm{k}) = 0\big\}\end{aligned} \tag{17}$$

Due to its dependency on ω_k, the MTPV hyperbola is moving in the $(i_\mathrm{s}^d, i_\mathrm{s}^q)$-plane (see light blue lines ——in Fig. 1).

C. Maximum-Torque-per-Flux (MTPF) hyperbola (with L_m)

An alternative to the MTPV strategy is the MTPF strategy. Nevertheless, it yields reference currents with larger magnitude (reduced efficiency) than those obtained from MTPV control. Due to this, MTPV should be used preferably (see Remark IV.6 in [13]). The MTPF optimization problem is formulated as follows

$$\max_{\boldsymbol{i}_\mathrm{s}^k\in\mathbb{S}} -\|\boldsymbol{\psi}_\mathrm{s}^k(\boldsymbol{i}_\mathrm{s}^k)\|^2 \text{s.t. } m_\mathrm{m}(\boldsymbol{i}_\mathrm{s}^k) = (\boldsymbol{i}_\mathrm{s}^k)^\top \boldsymbol{T}\boldsymbol{i}_\mathrm{s}^k + 2\boldsymbol{t}^\top(\boldsymbol{i}_\mathrm{s}^k) \stackrel{!}{=} m_{\mathrm{m,ref}} \tag{18}$$

with $\mathbb{S} := \mathbb{V}(\omega_\mathrm{k},\hat{u}_\mathrm{max}) \cap \mathbb{I}(\hat{\imath}_\mathrm{max})$. Its solution, the MTPF hyperbola (see gray line ——in Fig. 1) is implicitly given by the quadric (for details see [13])

$$\mathbb{MTPF} := \big\{\, \boldsymbol{i}_\mathrm{s}^k \in \mathbb{R}^2 \;\big|\; (\boldsymbol{i}_\mathrm{s}^k)^\top \boldsymbol{M}_\mathrm{F}\, \boldsymbol{i}_\mathrm{s}^k + 2\,\boldsymbol{m}_\mathrm{F}^\top \boldsymbol{i}_\mathrm{s}^k + \mu_\mathrm{F} = 0\big\}, \tag{19}$$

which does *not* depend on the angular velocity ω_k (in contrast to the MTPV hyperbola (17)), since

$$\left.\begin{aligned}\boldsymbol{M}_\mathrm{F} &:= \begin{bmatrix} m_\mathrm{F}^{11}, & m_\mathrm{F}^{12} \\ m_\mathrm{F}^{12}, & m_\mathrm{F}^{22}\end{bmatrix} = \boldsymbol{M}_\mathrm{F}^\top \\ \boldsymbol{m}_\mathrm{F} &:= \tfrac{3}{2}n_\mathrm{p}\begin{pmatrix} \big(2(L_\mathrm{s}^d)^2 - L_\mathrm{s}^d L_\mathrm{s}^q + 3L_\mathrm{m}^2\big)\frac{\psi_\mathrm{pm}^d}{4} + L_\mathrm{m}(L_\mathrm{s}^d + L_\mathrm{s}^q)\frac{\psi_\mathrm{pm}^q}{2} \\ L_\mathrm{m}(L_\mathrm{s}^d + L_\mathrm{s}^q)\frac{\psi_\mathrm{pm}^d}{2} + \big(2(L_\mathrm{s}^q)^2 - L_\mathrm{s}^d L_\mathrm{s}^q + 3L_\mathrm{m}^2\big)\frac{\psi_\mathrm{pm}^q}{4}\end{pmatrix}, \\ \mu_\mathrm{F} &:= \tfrac{3}{4}n_\mathrm{p}\Big[L_\mathrm{s}^d(\psi_\mathrm{pm}^d)^2 + 2L_\mathrm{m}\psi_\mathrm{pm}^d\psi_\mathrm{pm}^q + L_\mathrm{s}^q(\psi_\mathrm{pm}^q)^2\Big],\end{aligned}\right\} \tag{20}$$

and $m_\mathrm{F}^{11} = \frac{3}{2}n_\mathrm{p}\big[(\frac{L_\mathrm{s}^d - L_\mathrm{s}^q}{2}\big((L_\mathrm{s}^d)^2 + L_\mathrm{m}^2\big) + L_\mathrm{m}^2\big(L_\mathrm{s}^d + L_\mathrm{s}^q\big)\big]$, $m_\mathrm{F}^{12} = \frac{3}{2}n_\mathrm{p}\big[\frac{L_\mathrm{m}}{2}\big((L_\mathrm{s}^d)^2 + (L_\mathrm{s}^q)^2 + 2L_\mathrm{m}^2\big)\big]$ and $m_\mathrm{F}^{22} = \frac{3}{2}n_\mathrm{p}\big[-\frac{L_\mathrm{s}^d - L_\mathrm{s}^q}{2}\big((L_\mathrm{s}^q)^2 + L_\mathrm{m}^2\big) + L_\mathrm{m}^2\big(L_\mathrm{s}^d + L_\mathrm{s}^q\big)\big]$ do *not* depend on the electric angular velocity ω_k, respectively.

D. Analytical solutions of the optimal reference current vectors for MTPC, MTPV and MTPF

Due to space constraints, the derivation is not shown in this paper. The principle idea is based on the reformulation of the respective optimization problem as Lagrangian by introducing a Lagrangian multiplier $\lambda \in \mathbb{C}$ to account for the respective equality constraints. The solution of the Lagrangian depends on the roots of a fourth-order polynomial in λ (for details see [13]). The four roots can also be computed analytically (see [13, Appendix A]). The analytical expressions for the optimal reference current vectors are finally given as follows:

• **Maximum-Torque-per-Current (MTPC):** Solving the optimization problem in (14) by invoking the Lagrangian multiplier $\lambda \in \mathbb{C}$ to account for the equality constraint yields a fourth-order polynomial in λ (see Appendix A in [13]) and, with optimal Lagrangian multiplier $\lambda^\star$ (a real root of the fourth-order polynomial), the optimal reference current vector can be computed by

$$\boxed{\boldsymbol{i}_\mathrm{s,ref}^{k,\mathrm{MTPC}}(\lambda^\star) := -\big[\lambda^\star\,\boldsymbol{T} - \boldsymbol{I}_2\big]^{-1}\lambda^\star\,\boldsymbol{t},} \tag{21}$$

where $\boldsymbol{T}$ and $\boldsymbol{t}$ are as in (7).

• **Maximum-Torque-per-Voltage (MTPV)**: During MTPV operation, the voltage constraint is the most limiting factor and the reference torque is not feasible anymore. Therefore, the maximally feasible torque under the voltage constraint shall be produced. The general optimization problem (5) becomes

$$\begin{aligned}\boldsymbol{i}_\mathrm{s,ref}^{k,\mathrm{MTPV}} := \arg\max\nolimits_{\boldsymbol{i}_\mathrm{s}^k} \operatorname{sign}(m_\mathrm{m,ref})\, \overbrace{\Big((\boldsymbol{i}_\mathrm{s}^k)^\top \boldsymbol{T}\boldsymbol{i}_\mathrm{s}^k + 2\boldsymbol{t}^\top(\boldsymbol{i}_\mathrm{s}^k)\Big)}^{=m_\mathrm{m}(\boldsymbol{i}_\mathrm{s}^k)} \\ \text{s.t. } \boldsymbol{V}(\omega_\mathrm{k}) + 2\boldsymbol{v}(\omega_\mathrm{k})^\top \boldsymbol{i}_\mathrm{s}^k + \nu(\omega_\mathrm{k},\hat{u}_\mathrm{max}) = 0.\end{aligned}$$

It solution is given by (see Appendix A in [13])

$$\boldsymbol{i}_{\mathrm{s,ref}}^{k,\mathrm{MTPV}}(\lambda^\star) := -\Big[\lambda^\star \boldsymbol{V}(\omega_\mathrm{k}) + \mathrm{sign}(m_{\mathrm{m,ref}})\boldsymbol{T}\Big]^{-1}\Big(\lambda^\star \boldsymbol{v}(\omega_\mathrm{k}) + \mathrm{sign}(m_{\mathrm{m,ref}})\boldsymbol{t}\Big),$$

where $\boldsymbol{V}(\omega_\mathrm{k})$ and $\boldsymbol{v}(\omega_\mathrm{k})$, and $\boldsymbol{T}$ and $\boldsymbol{t}$ are as in (9) and (7), respectively.

• **Maximum-Torque-per-Flux (MTPF)**: During MTPF operation (as simplified alternative to MTPV), the voltage constraint is again the most limiting factor and the optimal reference current vector is obtained by the intersection of MTPF hyperbola $\mathbb{MTPF}$ as in (19) and voltage ellipse $\partial\mathbb{V}(\omega_\mathrm{k}, \hat{u}_{\max})$ as in (17), i.e.

$$\boldsymbol{i}_{\mathrm{s,ref}}^{k,\mathrm{MTPF}}(\lambda^\star) := -2\left[\frac{\boldsymbol{M}_\mathrm{F}}{\mu_\mathrm{F}} - \frac{\boldsymbol{V}(\omega_\mathrm{k})}{\nu(\omega_\mathrm{k}, \hat{u}_{\max})} - \lambda^\star \boldsymbol{J}\right]^{-1}\left(\frac{\boldsymbol{m}_\mathrm{F}}{\mu_\mathrm{F}} - \frac{\boldsymbol{v}(\omega_\mathrm{k})}{\nu(\omega_\mathrm{k}, \hat{u}_{\max})}\right),$$

where $\lambda^\star$ is one of the (real) roots of the fourth-order polynomials given in Equation (67) in [13, Appendix D].

Remark III.2 (Optimal reference currents for reluctance synchronous machines (RSMs))**.** *The analytical solutions for RSMs can be computed in a similar way as shown above; however, for RSMs, all quadrics simplify due to the missing permanent magnet, i.e.* $\psi_{\mathrm{pm}}^d = \psi_{\mathrm{pm}}^q = 0$*. The vectors* $\boldsymbol{t} = \boldsymbol{v}(\omega_\mathrm{k}) = \boldsymbol{f} = \boldsymbol{m}_\mathrm{C} = \boldsymbol{m}_\mathrm{V}(\omega_\mathrm{k}) = \boldsymbol{m}_\mathrm{F} = \boldsymbol{0}_2$ *and scalars* $\phi = \mu_\mathrm{V}(\omega_\mathrm{k}) = \mu_\mathrm{F} = 0$ *of torque hyperbola* (8)*, voltage ellipse* (10)*, flux norm* (12)*, MTPC hyperbola* (15)*, MTPV hyperbola* (17) *and MTPF hyperbola* (19) *become zero (see also* (7)*,* (9)*, and* (13)*), respectively. Therefore, all quadrics must be shifted by some (arbitrary)* $\boldsymbol{x}_\mathrm{s} \neq \boldsymbol{0}_2$ *by substituting* $\boldsymbol{i}_\mathrm{s}^k$ *by* $\boldsymbol{i}_\mathrm{s}^k := \bar{\boldsymbol{i}}_\mathrm{s}^k + \boldsymbol{x}_\mathrm{s}$ *(for more details see [13, Remark IV.8]).*

E. Graphical illustration

In Fig. 1, for a small $400\,\mathrm{W}$ IPMSM with the parameters $R_\mathrm{s} = 20\,\Omega$, $L_\mathrm{s}^d = 6 \cdot 10^{-2}\,\mathrm{H}$, $L_\mathrm{s}^q = 8 \cdot 10^{-2}\,\mathrm{H}, L_\mathrm{m} = 0.5 \cdot 10^{-3}\,\mathrm{H}, \boldsymbol{\psi}_{\mathrm{pm}}^k = (\psi_{\mathrm{pm}}, 0)^\top = (0.23\,\mathrm{Wb}, 0)^\top$ and $n_\mathrm{p} = 3$, the MTPC and MTPV strategy are illustrated for the positive reference torque $m_{\mathrm{m,ref}} = 3.35\,\mathrm{N\,m}$, the voltage limit $\hat{u}_{\max} = 600\,\mathrm{V}$ and the current limit $\hat{\imath}_{\max} = 5\,\mathrm{A}$. The illustrated optimal feedforward torque operation strategies are MTPC in Fig. 1a and MTPV in Fig. 1b. The respective optimal operation points, with their (optimal) reference current vectors $\boldsymbol{i}_{\mathrm{s,ref}}^k = (i_{\mathrm{s,ref}}^d, i_{\mathrm{s,ref}}^q)^\top$, are marked by ★ and correspond to the intersection of (a) $\mathbb{MTPC} \cap \mathbb{T}(m_{\mathrm{m,ref}})$ for MTPC in Fig. 1a and (b) $\mathbb{MTPV} \cap \partial\mathbb{V}(\omega_\mathrm{k}, \hat{u}_{\max})$ for MTPV in Fig. 1b, respectively. For increasing electric angular velocities $\omega_\mathrm{k} \in \{1, 3\}\omega_{\mathrm{k,nom}}$ (where $\omega_{\mathrm{k,nom}}$ is the nominal electric angular velocity), the MTPV hyperbola is approaching the MTPF hyperbola (see also [13, Remark IV.6]) and the voltage ellipse is shrinking; whereas the current circle, MTPC hyperbola, torque hyperbola and MTPF hyperbola are independent of the angular velocity and, hence, do *not* change in the three plots. Moreover, Fig. 1a & b illustrate the impact of neglecting (i) stator resistance (i.e. $R_\mathrm{s} = 0$: dashed line), (ii) mutual inductance (i.e. $L_\mathrm{m} = 0$: dash-dotted line) or (iii) both (i.e. $R_\mathrm{s} = L_\mathrm{m} = 0$: dotted line) on the shape of MTPC, MTPV, MTPF and torque hyperbolas and the voltage ellipse. It is easy to see that neglecting stator resistance, mutual inductance or both would lead to different (and wrong) intersection points and, hence, *not* optimal operation points with *reduced efficiency*. For example, the impact of neglecting stator resistance, mutual inductance or both on the shape, size and orientation of the voltage ellipse is obvious. Concluding, both parameters, R_s and L_m must *not* be neglected.

IV. Implementation and Measurement Results

The theoretical derivations are validated by the following real-time implementation of the proposed analytical MTPC strategy with the computation of the MTPC reference current vector $\boldsymbol{i}_{\mathrm{s,ref}}^k = \boldsymbol{i}_{\mathrm{s,ref}}^{k,\mathrm{MTPC}}$ as in (21) and its application to a highly nonlinear custom-built $9.6\,\mathrm{kW}$ RSM (Courtesy of Prof. Maarten Kamper, Stellenbosch University, ZA) with the parameters $R_\mathrm{s} = 0.4\,\Omega$, $\omega_{\mathrm{k,nom}} = \frac{2\pi}{60\,\mathrm{s}} \cdot 1\,500\,\mathrm{rpm} = 157.07\,\frac{\mathrm{rad}}{\mathrm{s}}$, $m_{\mathrm{m,nom}} = 61\,\mathrm{N\,m}$, $\hat{\imath}_{\max} = 29.7\,\mathrm{A}$, and $\hat{u}_{\max} = 590\,\mathrm{V}$, and the nonlinear (current-dependent) *differential* inductances L_s^d, L_s^q and L_m, as shown in Fig. 2, computed by numerical differentiation of the flux maps (not shown; obtained by measurements or FEA) with respect to the currents. The overall laboratory setup comprises a dSPACE real-time system, two $22\,\mathrm{kW}$ SEW inverters in back-to-back configuration sharing a common DC-link, a HOST-PC running MATLAB/Simulink for rapid-prototyping & data acquisition, the custom-built $9.6\,\mathrm{kW}$ RSM and a $14.5\,\mathrm{kW}$ SEW PMSM to regulate the mechanical speed. The experiments were conducted for MTPC operation in motor mode (constant reference torque) at constant speed $\omega_\mathrm{k} \approx \omega_{\mathrm{k,nom}}$. The reference torque $m_{\mathrm{m,ref}}$ was increased stepwise by increments of $1\,\mathrm{N\,m}$ from zero to nominal torque $m_{\mathrm{m,nom}}$ and held constant at each step for two seconds. The nonlinear flux linkages and inductances (as in Fig. 2) were tracked online (using look-up tables) and fed into to the feedforward torque controller at each sampling instant. The measurement results of the analytical MTPC approach were compared with the numerically calculated reference currents. To be able to express the nonlinear RSM dynamics in the form (1) with affine flux linkage (2), the nonlinear flux linkage of the RSM was linearized online (at each sampling instant). The computed reference currents of both, the numerical and the analytical torque feedforward controller, are shown in Cartesian coordinates and polar coordinates in Fig. 3a and Fig. 3b, respectively. Both solutions give almost identical reference currents. The numerical solution shows an unexpected shape (dip) for lower currents (due to a deteriorated interpolation/accuracy and/or a numerical instability of the numerical solver) and, for higher currents, gives reference vectors with larger magnitudes leading to higher copper losses than the analytical approach. The analytical and numerical solution (for the roots of the fourth-order polynomial) are obtained on average with execution times of $\mu_a = 7.23 \cdot 10^{-6}\,\mathrm{s}$ and $\mu_n = 43.4 \cdot 10^{-6}\,\mathrm{s}$, respectively. Concluding, the analytical

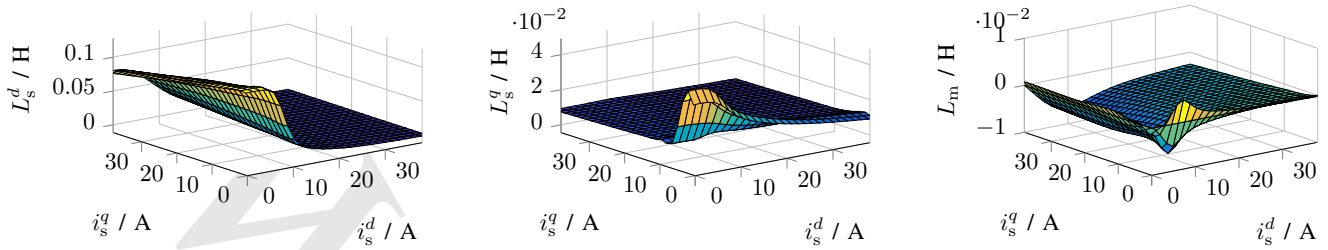

(a) *Self inductance* $L_s^d := \frac{d\psi_s^d}{di_s^d}$. (b) *Self inductance* $L_s^q := \frac{d\psi_s^q}{di_s^q}$. (c) *Mutual inductance* $L_m := \frac{d\psi_s^d}{di_s^q} = \frac{d\psi_s^q}{di_s^d}$.

Fig. 2: *Nonlinear inductances of the custom-built* 9.6 kW *RSM (inductances shown in the first quadrant, i.e.* $i_s^d \geq 0$ *and* $i_s^q \geq 0$*).*

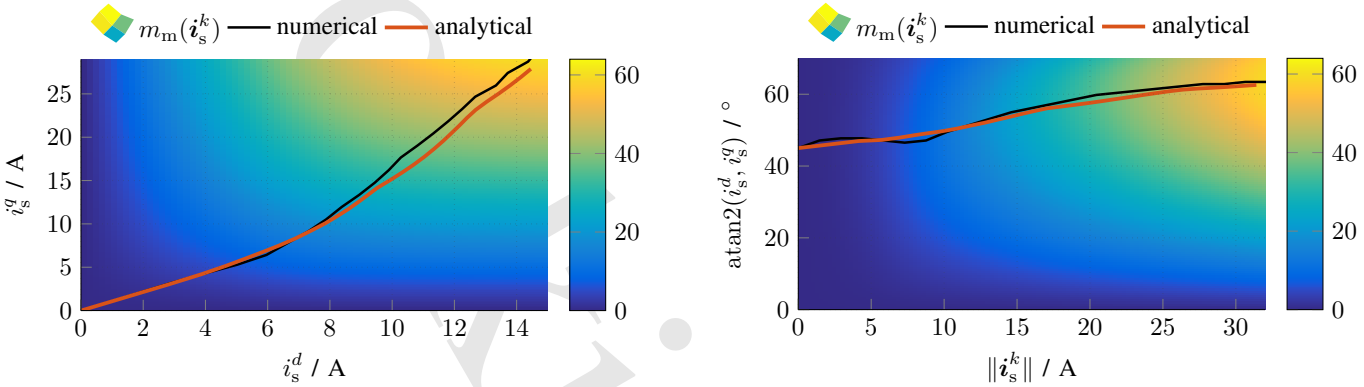

(a) *Computed reference currents in Cartesian coordinates.* (b) *Computed reference currents in polar coordinates.*

Fig. 3: *Measurement results for a nonlinear custom-build* 9.6 kW *RSM at* 150 $\frac{\text{rad}}{\text{s}}$*: Comparison of the optimal reference currents* $i_{s,ref}^k = (i_{s,ref}^d, i_{s,ref}^q)^\top$ *for MTPC operation computed by the conventional numerical and the proposed analytical method.*

method is about six times faster, and gives a more accurate solution with higher efficiency than the numerical method.

Acknowledgement

This project received funding from the European Union's Horizon 2020 research and innovation programme under the Marie Sklodowska-Curie grant agreement No. 642682 & from the Bavarian Ministry for Eduction, Culture, Science & Art.

References

[1] A. de Almeida, F. Ferreira, and J. Fong, "Ieee industry applications magazine," *Industry Application Magazine*, vol. 17, no. 1, pp. 12–19, 2011.

[2] I. Boldea, L. Tutelea, Lucian N. Parsa, and D. Dorrell, "Automotive electric propulsion systems with reduced or no permanent magnets: An overview," *IEEE Transactions on Industrial Electronics*, vol. 61, no. 10, pp. 5696–5711, 2014.

[3] E. Schmidt, "Synchronous reluctance machines with high-anisotropy rotors – comparison of their operational characteristics," in *Proceedings of the Australasian Universities Power Engineering Conference*, pp. 1–6, 2014.

[4] M. Tursini, E. Chiricozzi, and R. Petrella, "Feedforward flux-weakening control of surface-mounted permanent-magnet synchronous motors accounting for resistive voltage drop," *IEEE Transactions on Industrial Electronics*, vol. 57, no. 11, pp. 440–448, 2010.

[5] S.-Y. Jung, J. Hong, and K. Nam, "Current minimizing torque control of the IPMSM using Ferrari's method," *IEEE Transactions on Power Electronics*, vol. 28, no. 12, pp. 5603–5617, 2013.

[6] M. Preindl and S. Bolognani, "Optimal state reference computation with constrained MTPA Criterion for PM motor drives," *IEEE Transactions on Power Electronics*, vol. 30, no. 8, pp. 4524–4535, 2015.

[7] J. Lemmens, P. Vanassche, and J. Driesen, "PMSM drive current and voltage limiting as a constraint optimal control problem," *IEEE Journal of Emerging and Selected Topics in Power Electronics*, vol. 3, no. 2, pp. 326–338, 2015.

[8] L. Horlbeck and C. Hackl, "Analytical solution for the MTPV hyperbola including the stator resistance," in *Proceedings of the IEEE International Conference on Industrial Technology (ICIT 2016)*, (Taipei, Taiwan), pp. 1060–1067, 2016.

[9] R. Ni, D. Xu, G. Wang, L. Ding, G. Zhang, and L. Qu, "Maximum efficiency per ampere control of permanent-magnet synchronous machines," *IEEE Transactions on Industrial Electronics*, vol. 62, no. 4, pp. 2135–2143, 2015.

[10] J. Ahn, S.-B. Lim, K.-C. Kim, J. Lee, J.-H. Choi, S. Kim, and J.-P. Hong, "Field weakening control of synchronous reluctance motor for electric power steering," *IET Electric Power Applications*, vol. 1, no. 4, pp. 565–570, 2007.

[11] H. Eldeeb, C. M. Hackl, and J. Kullick, "Efficient operation of anisotropic synchronous machines for wind energy systems," in *Proceedings of the 6th edition of the conference "The Science of Making Torque from Wind" (TORQUE 2016)*, Open access Journal of Physics: Conference Series 753, (Munich, Germany), 2016.

[12] C. M. Hackl, M. J. Kamper, J. Kullick, and J. Mitchell, "Current control of reluctance synchronous machines with online adjustment of the controller parameters," in *Proceedings of the 2016 IEEE International Symposium on Industrial Electronics (ISIE 2016)*, (Santa Clara, CA, USA), pp. 153–160, 2016.

[13] H. Eldeeb, C. M. Hackl, L. Horlbeck, and J. Kullick, "On the optimal feedforward torque control problem of anisotropic synchronous machines: Quadrics, quartics and analytical solutions," *arXiv:1611.01629 (see https://arxiv.org/pdf/1611.01629)*, 2016.